

Path-Integral Computation of the Low-Temperature Properties of Liquid ^4He

D. M. Ceperley and E. L. Pollock

Lawrence Livermore National Laboratory, University of California, Livermore, California 94550

(Received 28 October 1985)

Discretized path-integral computations of the energy and radial distribution function of ^4He in good accord with experiment are presented for temperatures down to 1 K at saturated vapor pressure. Results for the single-particle density matrix, momentum distribution, and condensate fraction agree at the lowest temperature with previous ground-state calculations.

PACS numbers: 67.40.-w

The unusual properties of liquid ^4He at low temperature were attributed to Bose-Einstein condensation by London in 1938.¹ The strength of the pair interaction between helium atoms, however, has so far prevented a first-principles study of this transition in ^4He . In this Letter we present a Monte Carlo discretized path-integral computation of the density matrix for liquid ^4He for temperatures spanning this transition which reproduces many of the experimental results and is in principle capable of arbitrary accuracy. We have assumed that the atoms interact via the Aziz pair potential.²

The calculations for the many-body density matrix,³

$$\rho(R, R'; \beta) = \langle R | e^{-\beta H} | R' \rangle, \quad (1)$$

from which all equilibrium properties can be obtained, are based on the identity³

$$\rho(R, R'; \beta) = \int \cdots \int \rho(R, R_1; \tau) \rho(R_1, R_2; \tau) \cdots \rho(R_{M-1}, R'; \tau) dR_1 \cdots dR_{M-1}, \quad (2)$$

where $\tau = \beta/M$, $M > 1$, and the R variables denote points in the $3N$ -dimensional coordinate space. If an accurate many-body density matrix is known at some high temperature corresponding to τ then Eq. (2) allows its calculation at a lower temperature $T = 1/Mk\tau$. The density matrix for Bose systems is obtained by summing over all permutations of particle labels:

$$\rho_B(R, R'; \beta) = (N!)^{-1} \sum_P \rho(R, PR'; \beta). \quad (3)$$

Both the integral over paths and the sum over permutations are performed by a generalization of the Metropolis

TABLE I. Computed potential and kinetic energies for various temperatures at SVP. The statistical uncertainty in the potential energy is about 0.04 and 0.08 K in the kinetic energy. The densities used are based on Crawford.^a The last six columns give the first three zeros and extremal values of the pair correlation function $h(r) = g(r) - 1$. The last row at 2.0 K is for distinguishable particles.

$T(^{\circ}\text{K})$	$\rho(\text{\AA}^{-3})$	$\langle U \rangle / N (^{\circ}\text{K})$	$\langle K \rangle / N (^{\circ}\text{K})$	$r_1(\text{\AA})$	$r_2(\text{\AA})$	$r_3(\text{\AA})$	h_1	h_2	h_3
4.0	.01932	-18.91	15.65	2.973	4.583	6.271	.356	-.113	.040
3.333	.02072	-20.38	16.00	2.962	4.552	6.240	.369	-.126	.050
2.857	.02142	-21.14	15.99	2.950	4.537	6.234	.381	-.134	.055
2.50	.02179	-21.52	15.90	2.948	4.533	6.220	.383	-.136	.059
2.353	.02191	-21.60	15.75	2.945	4.526	6.205	.382	-.136	.060
2.222	.02197	-21.70	15.89	2.945	4.526	6.205	.382	-.139	.061
2.105	.02194	-21.57	15.10	2.940	4.522	6.205	.374	-.131	.055
2.0	.02191	-21.57	15.05	2.942	4.525	6.211	.377	-.132	.056
1.818	.02186	-21.44	14.71	2.939	4.526	6.209	.369	-.127	.053
1.600	.02183	-21.39	14.40	2.938	4.520	6.213	.368	-.124	.051
1.379	.02182	-21.35	14.23	2.937	4.515	6.206	.366	-.123	.050
1.1765	.02182	-21.35	14.17	2.938	4.520	6.212	.366	-.123	.050
2.0	.02191	-21.75	16.24	2.950	4.535	6.205	.385	-.140	.064

^aReference 5.

Monte Carlo method. A discussion of how this is implemented for distinguishable particles is given by Pollock and Ceperley.⁴ In the extension of this work to bosons several new techniques were required which will be described in detail elsewhere, but before presenting our results we briefly mention two of the most important.

First (as in Ref. 4) the many-body density matrix at high temperature in Eq. (2) is taken as a product of one- and two-body density matrices which is exact in the high-temperature limit. Here we have used the full two-body density matrix rather than the "end point" approximation of earlier work. This is more accurate and allows larger values of τ (smaller M) to be used in Eq. (2). The high-temperature density matrix used was typically for a temperature of 40 K and thus paths of about twenty steps were needed for computations near T_λ . Had we been interested in only the structural properties rather than, for example, the kinetic energy, steps corresponding to 20 K or less would have sufficed. We have checked the adequacy of the step size by rerunning selected points using 80-K steps. A thorough convergence study of the earlier method was done in Ref. 4.

Secondly, a new method was used to construct trial paths for the multiparticle moves necessary in the sampling of the permutations of Eq. (3). The particular particles (here as many as four) for which permutation changes are attempted at one Monte Carlo move are initially selected on the basis of the free-particle density matrix. New trial paths are then generated by a "bisection method" which first generates new midpoints for paths and then new midpoints for the remaining halves and so on, with the possibility of rejecting the new paths at any stage in the construction. For permutations this is more efficient than the previous method of sequentially generating new paths step by step since now improbable paths may be rejected at an early stage in their construction, thus allowing many more trial moves for a given amount of computer time. The rejection step ensures that the accepted permutations and paths reflect the correct density matrix and not our initial guesses. Extensive tests of the convergence of the distribution of permutations were carried out.

Table I lists some of the temperatures and densities at saturated vapor pressure (SVP) along with the potential and kinetic energy and some structural properties where computations were done. The computed energy and specific heat as functions of temperature at SVP near T_λ are compared with experiment in Fig. 1. The simulations are for a periodic system of 64 atoms and each run takes about one hour on the Cray-1. The finite number of particles used in these simulations apparently depresses the computed energy in the temperature region $2.1 \text{ K} < T < 3 \text{ K}$.

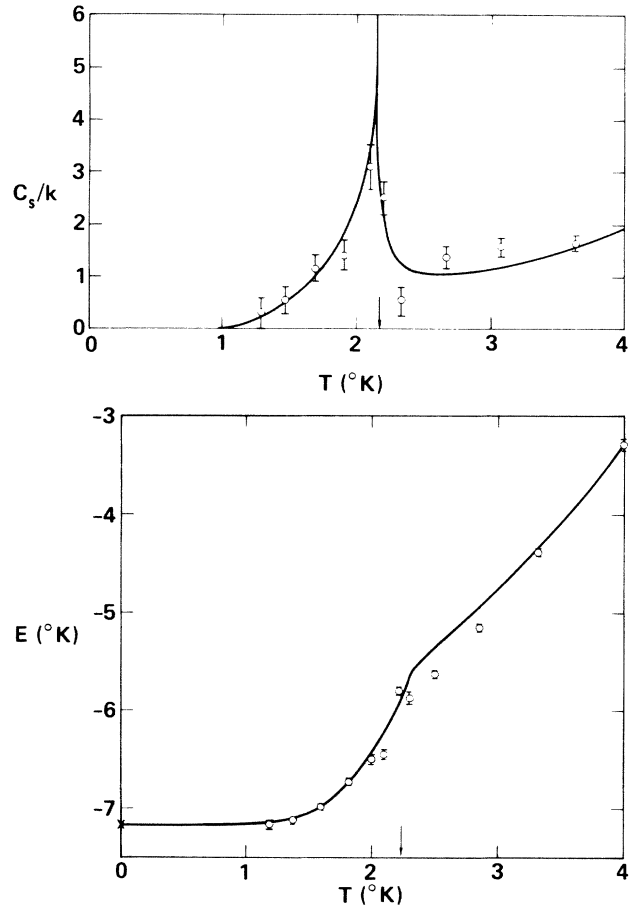


FIG. 1. Energy and specific heat at SVP near T_λ . The solid lines are the experimental values. [The energy was taken from Ref. 5 and the specific heat from Wilks (Ref. 6).] The simulation results for the specific heat were obtained by a differencing of the energy values. The energy computed from ground-state simulations (Ref. 7) is denoted by the cross. The experimental value for T_λ (2.17 K) is indicated by the arrow.

The effect of Bose statistics on the radial distribution function, $g(r)$, is small as shown at $T = 2.0$ K SVP in Fig. 2(a) where the neutron-scattering results⁸ are compared with the present simulation. The dashed line shown at the first peak and first minimum is for distinguishable particles [only the identity permutation is allowed in Eq. (3)] and shows the slightly increased spatial ordering attributed, via the uncertainty principle, to the decreased ordering in momentum space when the condensate is suppressed. Similar good agreement is obtained between the computed radial distribution and structure functions and the available neutron and x-ray⁹ scattering data at other temperatures and pressures in the liquid phase.

The single-particle momentum distribution, $n(k)$, is the Fourier transform of the single-particle off-

diagonal density matrix, $n(r)$ ¹⁰:

$$n(r) = \frac{\int \rho_B(r_1, r_2, \dots, r_n, r_1+r, r_2, \dots, r_n; \beta) dr_1 \cdots dr_n}{\int \rho_B(r_1, r_2, \dots, r_n, r_1, r_2, \dots, r_n; \beta) dr_1 \cdots dr_n}, \quad (4)$$

which in terms of path integrals corresponds to one open path beginning at r_1 and ending at r_1+r . (Here the r_i are the coordinates of atom i .) At temperatures well above T_λ where only the identity permutation is important, this open path involves only one particle and is restricted to a distance on the order of the thermal wavelength, $\hbar/(2mkT)^{1/2}$. This is primarily due to the free-particle part of the density matrix somewhat modified by many-body effects. Below T_λ this open path may involve a long cyclic permutation of many particles and the end-to-end distance will become macroscopic. The $n(r)$ in Fig. 2(b) shows this change in character on going through the transition.¹² The initial curvature is proportional to the kinetic energy and the value at large r is the fraction of particles in the zero-momentum state, the condensate. Figure 3(a) shows this condensate fraction as a function of temperature. The condensate fractions plotted there are obtained by our assuming $n(r)$ to be constant beyond 5 Å and averaging the values between 5 and 7 Å to obtain

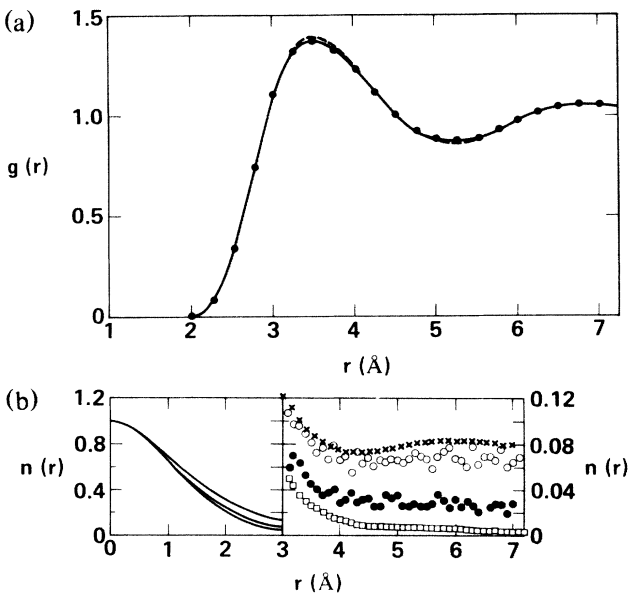


FIG. 2. (a) Radial distribution function for ${}^4\text{He}$ at 2 K and SVP. The solid line is the neutron-scattering result (Ref. 8). The circles are simulation results for bosons and the dashed line is for distinguishable particles. (b) Single-particle off-diagonal density matrix at 1.18 K (top curve and open circles), 2.22 K (middle curve and closed circles), and 3.33 K (lower curve and open squares). Beyond 3 Å the vertical axis is enlarged by 10 times and the interpolating curves are omitted. The crosses denote the ground-state results (Ref. 11) which are indistinguishable from the $T = 1.18$ K results for $r < 3$ Å on this graph.

$n_0(T)$. Near T_λ $n(r)$ reaches its asymptotic value slowly and this procedure, because of the relatively small system simulated and periodic boundary effects, is not reliable. For example we find an $n_0(T)$ value of 1.4% at 2.5 K, significantly above the experimental transition temperature. Larger systems must be considered to determine the condensate fraction near T_λ . The momentum distribution of the noncondensed par-

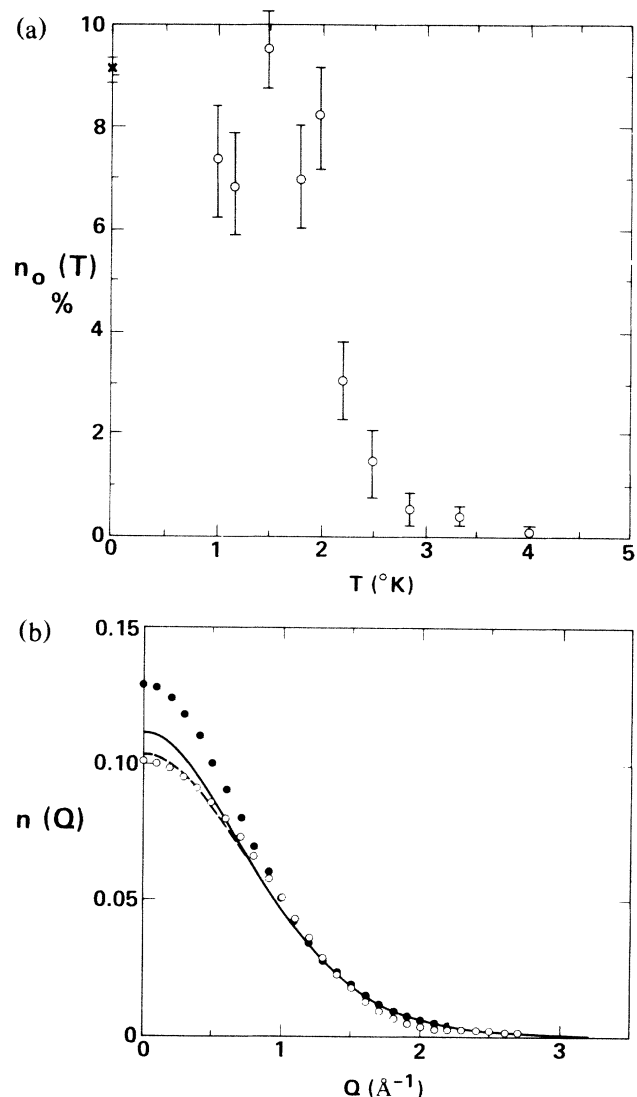


FIG. 3. (a) Percentage of atoms with zero momentum, $n_0(T)$, in ${}^4\text{He}$ at SVP. The indicated ground-state value is from Ref. 7. (b) Momentum distribution from simulations at temperatures of 3.33 K (solid curve), 2.22 K (dashed curve), 1.18 K (open circles), and for distinguishable particles at 2.22 K (solid circles).

ticles, Fig. 3(b), both is non-Gaussian and has a temperature-dependent shape. The present simulations are too noisy to test adequately the predicted low-momentum singularities in this distribution.¹³

In the past, estimates of the condensate fraction have been made¹⁴ based on the hypothesis of Hyland, Rowlands, and Cummings¹⁵ that the pair correlation function at large r has a constant shape below T_λ and is multiplied by $[1 - n_0(T)]^2$ (intuitively speaking the probability is that neither atom in the pair is in the condensate and thus spatially uniform). We can only test this at moderate values of r but an estimate of $n_0(T)$ based on the second maximum, h_3 , listed in Table I does not conflict with our results. Estimates based on the first minimum, h_2 , at smaller r seem definitely too small. Another intuitive estimate¹⁶ of $n_0(T)$ assumes the contribution of noncondensed atoms to the kinetic energy to be unchanged below T_λ where the condensate makes no contribution and thus the kinetic energy is proportional to $1 - n_0(T)$. Figure 3(b) suggests that this assumption is only approximate; nevertheless this estimate, using Table I, also accords with our results of the still-sizable error bars in the $n_0(T)$ estimates.

Efforts are under way to extend these simulations to larger systems and to determine other properties of ^4He .

This work was performed under the auspices of the U.S. Department of Energy by the Lawrence Livermore National Laboratory under Contract No. W-7405-ENG-48.

¹F. London, *Nature (London)* **141**, 643 (1938).

²R. A. Aziz, V. P. S. Nain, J. S. Carley, W. L. Taylor, and G. T. McConville, *J. Chem. Phys.* **70**, 4330 (1979).

³R. P. Feynman, *Statistical Mechanics* (Benjamin, Reading, Mass., 1972).

⁴E. L. Pollock and D. M. Ceperley, *Phys. Rev. B* **30**, 2555 (1984).

⁵R. K. Crawford, in *Rare Gas Solids*, edited by M. L. Klein and J. A. Venables (Academic, New York, 1976), Vol. 1, p. 663.

⁶J. Wilks, *Properties of Liquid and Solid Helium* (Clarendon, Oxford, 1967).

⁷M. H. Kalos, M. A. Lee, P. A. Whitlock, and G. V. Chester, *Phys. Rev. B* **24**, 115 (1981).

⁸E. C. Svensson, V. F. Sears, A. D. Woods, and P. Martel, *Phys. Rev. B* **21**, 3638 (1980).

⁹H. N. Robkoff and R. B. Hallock, *Phys. Rev. B* **24**, 159 (1981).

¹⁰O. Penrose and L. Onsager, *Phys. Rev.* **104**, 576 (1956).

¹¹P. A. Whitlock, private communication of work in progress. For values of r less than the de Broglie thermal wavelength the $n(r)$ from the finite-temperature simulations is of comparable accuracy with the ground-state result. At larger r it proved necessary actually to simulate a system with one open path, as described in the text, and as seen in Fig. 2(b) the scatter in the finite-temperature results is greater there.

¹²It is interesting to note that a formal correspondence between Bose-Einstein condensation and polymerization was noted over 35 years ago. W. H. Stockmayer and B. H. Zimm, *Annu. Rev. Phys. Chem.* **35**, 1 (1984), and references therein.

¹³A. Griffin, *Phys. Rev. B* **30**, 5057 (1984).

¹⁴V. F. Sears and E. C. Svensson, *Int. J. Quantum Chem.* **14**, 715 (1980).

¹⁵G. J. Hyland, G. Rowlands, and F. W. Cummings, *Phys. Lett.* **31A**, 465 (1970).

¹⁶V. F. Sears, *Phys. Rev. B* **28**, 5109 (1983).